

FINAL REPORT
February 24, 2017

**SELF-HEALING RENDERED PROTEIN BASED THERMOSETS FOR HIGH-VALUE
AUTOMOTIVE APPLICATIONS**

Principal Investigator(s): Srikanth Pilla, Assistant Professor
spilla@clmson.edu
Department of Automotive Engineering
4 Research Drive
Clemson University
Greenville, SC 29634
(864) 283-7216

Date Submitted: March 9, 2015

Project Start Date: June 1, 2015

Duration of Project: 18 months

Lay Summary:

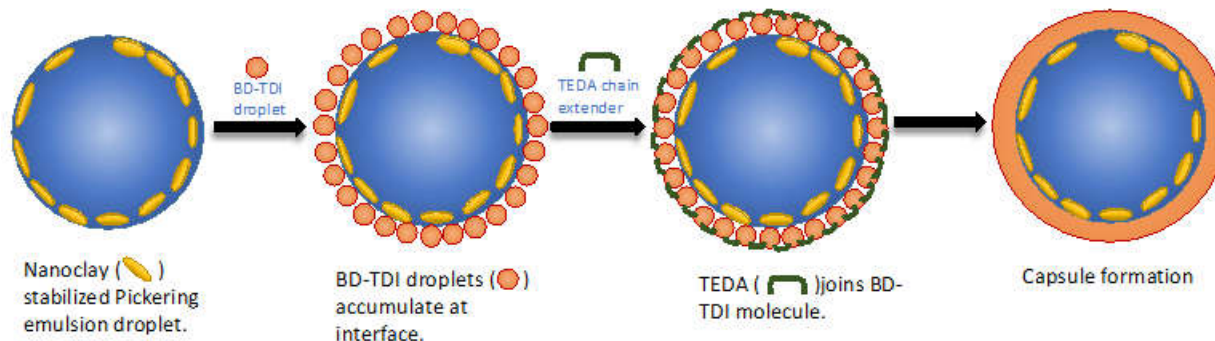
The project aims to enhance the overall service life of animal protein (AP)-based polymeric systems by imparting self-repairing capabilities via incorporation of microcapsules containing healing agents. This will involve the custom building of microcapsules that can carry hydrophilic healing materials targeted specifically for animal proteins and the introduction of the capsules into an animal protein based crosslinked polymeric systems.

Objectives: The overall objective of this study is to create a novel animal protein-based self-healing matrix for performance-oriented applications. This project will overcome a current challenge in self-healing research arena, viz. development of microcapsules that can enclose hydrophilic healing agent (e.g. formaldehyde), a critical component for the self-healing of animal protein based resins. The envisioned capsules should have a robust shell, proper dimension (50~100 micron) and lower permeability to serve as the micro-container.

Project Overview:

The project can be divided into three parts; **Part 1:** designing a novel, robust microcapsule that encompasses hydrophilic reagents. This is a recognized challenge and overcoming this will open up lots of opportunities in diverse fields. **Part 2:** Engineering an AP-based cross-linked polymeric matrix. As part of the previous phase of the funding, we evaluated the applicability AP to crosslink epoxy matrices. However, due to the incompatibility between the matrix and AP (due to the inherent hydrophilicity of AP), the trials were only moderately successful. However, leveraging the lessons learned, we continued the research and successfully developed a novel catalytic self-cross-linking strategy based on AP to create a cross-linked epoxy matrix. Part-2 was self-funded post the seed funding from ACREC in the first phase of project. **Part 3:** Incorporation of developed microcapsules into engineered AP crosslinked epoxy matrix and test self-healing possibilities. We envisage that the novel capsule architecture developed in the project and the new design of AP-assisted crosslinking strategy for epoxy matrices will generate high interest in AP and will lead to enhanced utilization of AP.

Part 1: Designing a novel microcapsule architecture: As an initial strategy, a facile diol-isocyanate reaction in water-in-oil inverse pickering method (**Scheme 1**) was used to prepare a capsule containing the healing agent.



Scheme 1. The mechanism of constructing self-healing capsules

The initial results showed facile capsule formation. Here, the diol (water phase) reacts with the isocyanate (oil phase) at the interface between oil and water to form the capsule shell which encapsulates the healing agent in the core of the capsule. The reaction readily resulted in capsule formation. However, the formed capsules were weak and highly unstable. For making the capsules more robust, a prerequisite for automotive applications, we reinforced (**Figure 1**) the capsule shell (wall) using various unmodified (Cloisite Ca⁺⁺) and hydrophobically modified organoclay platelets (Cloisite 10A, 15 and 20). The organically modified clays were prepared by ion-exchange reaction between sodium montmorillonite (Na-MMT) and ammonium surfactants. The formed capsules after the clay particle incorporation were more robust and could be isolated from solutions. We were also able to identify the most suitable clay particle and the optimum clay content to obtain the best capsule configuration (**Figure 1**). The next stage is to incorporate the formulated microcapsule in the AP-based epoxy matrix and evaluate its self-healing efficiency. This work is currently undergoing in the lab.

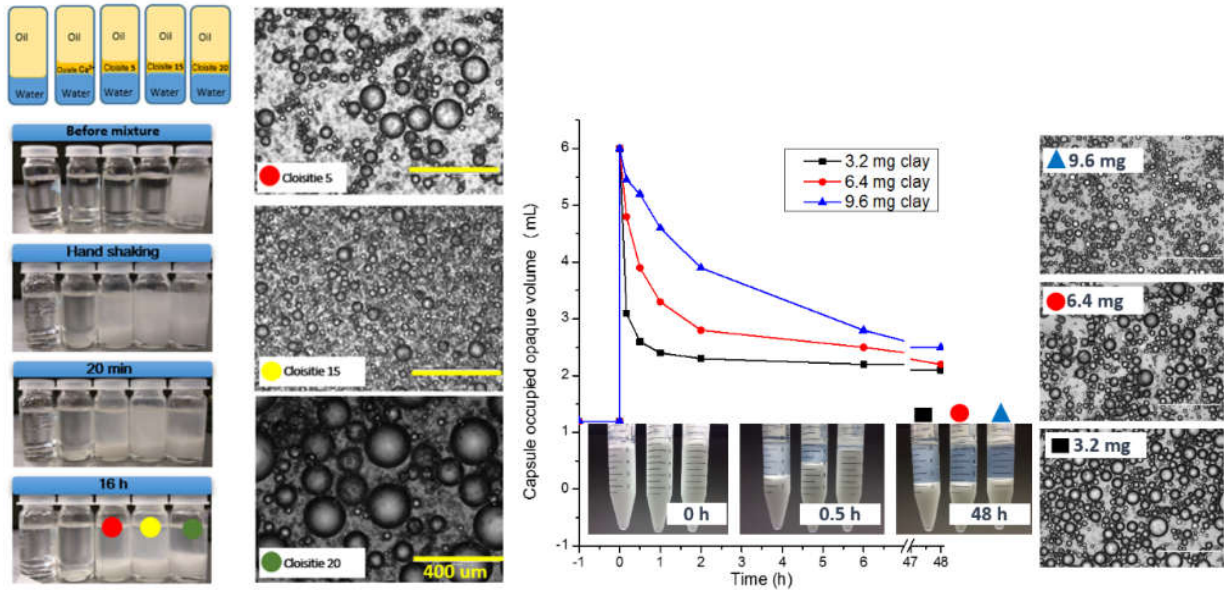


Figure 1. Optical microscope images of the organoclay stabilized Pickering emulsion before the addition of the isocyanate

Key points:

The organoclay stabilized capsules exhibited stability up to 16 h, indicating the efficient stabilization by organoclay. Moreover, unmodified nanoclay (Cloiste Ca⁺⁺) failed to stabilize the capsules indicating the essential role of the surface modification of clay in forming the Pickering emulsion. The size of the formed capsules intimately depended on the species and amount of the nanoclay added. For the purpose of self-healing, capsules with the diameters around 100 microns are reported favorable. Thus Cloiste 20 (3.2 mg to 6.4 mg) will be employed for future studies.

Optimization and testing the stability

Different parameters such as agitation speed, oil/water volume ratio, temperature, chemical component, etc. can modulate the morphology, size, and the strength of the capsule. Here, the synthesis process was optimized, and the results indicate that higher temperature (40°C), and concentration of the isocyanate/polyol is essential for capsule formation. An optimized molar ratio of PMPPI:TDI was determined. Compared with the pre-emulsion, a wide size distribution was observed in the final mix. The existence of smaller and larger capsules prepared after the interfacial reaction indicates that droplets break and coalesce during the reaction. Although several small capsules (<20 μm) exist, the major volume of the solution was encapsulated in bigger capsules (80~200 μm). We tested the stability of the capsules under different conditions (**Figure 2**). While the capsules were stable in the solution and moderately stable in air (dried powder), pipette tips were able to break them easily in the dried state.

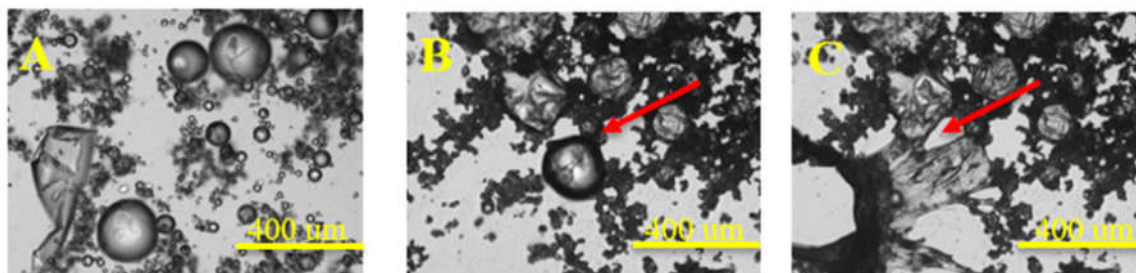


Figure 2. Stability of capsules under different conditions. The capsule in the solution (A), dried in the air (B), and torn by pipette tip (C).

Key points:

While the capsules formed at optimal conditions showed several smaller capsules, the majority of them had an average diameter <100 μm, and hence are ideal for self-healing applications. However, the capsules were easily broken by pipette tips, though they showed appreciable stability in solution and air. To apply for self-healing, the stability of the capsules should be enhanced. We are working on strategies to improve the stability of the capsules.

Confirmation of the presence of healing agent in the capsule

We used a fluorescent dye dispersed in water to confirm the ability of capsule to encompass the healing agent within its shell. Water soluble Rhodamine B dye was introduced into the capsule forming mixture resulting in the encapsulation of the dye. **Figure 3** clearly shows the formation of capsules and the fluorescence microscopic image confirmed the retaining of the dye inside the formed capsules. This proves that, when the capsules are reinforced to have higher stability, they can be used as containers for healing agents and can be used for self-healing applications.

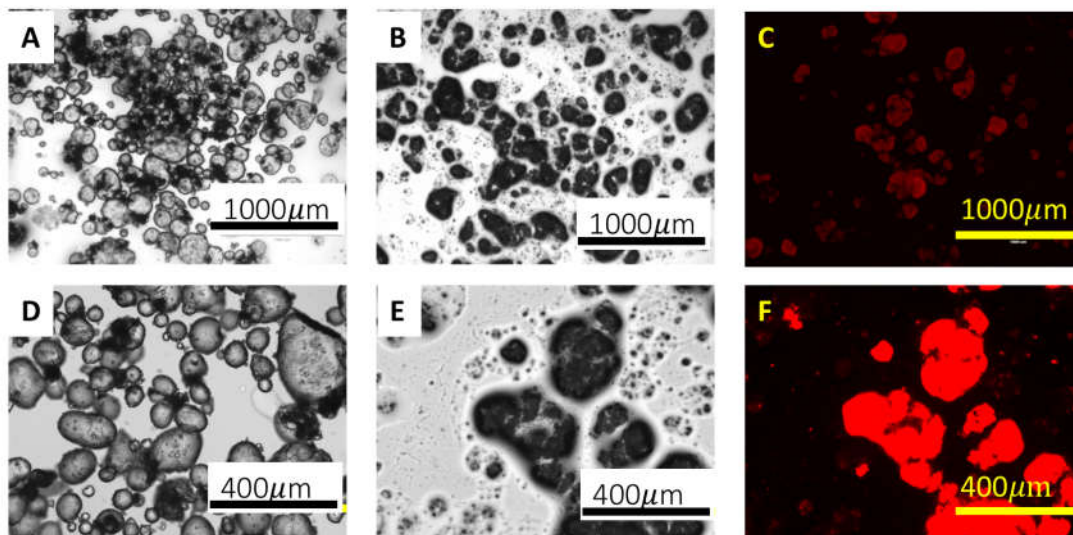


Figure 3. Optical and fluorescence microscopic image of capsule filled with dyes

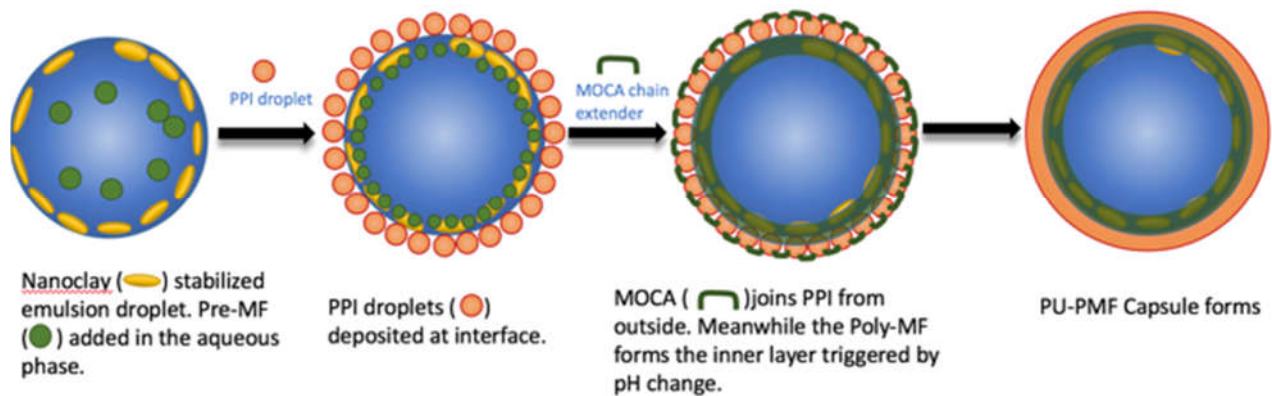
Development of microcapsules with bilayered walls

While the prepared capsules were moderately stable and were able to retain liquid payloads, they were not robust enough to incorporate them into a polymeric matrix. Moreover, they were unstable towards various processing techniques such as agitation, centrifuging, vortex, etc. Hence, a considerable enhancement in stability was required to employ them for self-healing applications. To reinforce the microcapsule, we developed a novel capsule formulation strategy called *“water-in-oil-in-oil” pre-emulsion strategy (Scheme 2)*. In this pathway, the shell forming material: e.g. the isocyanate, was confined and reacted in the middle oil layer. Using a middle layer, problems associated with previous shell formation such as a high concentration of chain extender and low concentration of the isocyanate was avoided. The capsule formation involved, two stages. In the first stage, the fabrication of an isocyanate-rich layer around the water droplet in the emulsion as the location of the shell formation reaction (**stage a**), where the shell formation takes place via the interfacial polymerization. The mechanical properties of the shell were reinforced by constructing an internal lining, by the concurrent PMF (poly(melamine-formaldehyde)) stiffening layer (**Stage b**). The permeability test showed that our capsules has very low permeability indicating the high utility to carry hydrophilic payloads such as formaldehyde in extreme condition and for long durations.

“Water-in-oil-in-oil (W/O/O)” emulsion technique

Stage a. PPI attachment and interlayer formation

We developed a facile and effective methodology to engineer an isocyanate enriched phase wrapping around each individual aqueous droplet. Such layer was achieved by adding polymeric isocyanate emulsion (PPI emulsion) to the Pickering pre-emulsion (template emulsion) discussed earlier. Driven by interfacial tension, PPI droplets gets embedded onto the surface of template emulsion. Subsequently, the PPI droplets merge together to form a coating layer. The addition of a chain extender into the continuous oil phase result in the formation of reinforcing layer on the microcapsule (**Scheme 2**).



Scheme 2. Mechanism of PU-PMF shell formation. PPI droplets migrate to the interface of template droplet where they fuse, spread and engulf template droplets to form isocyanate-rich layer as the location of the consequent PU shell-forming reaction

Characterization of the W/O/O architecture of capsule formation

Our conjecture is that PPI droplets get adsorbed onto the surface of the template water droplets which aids in the formation of the second wall. The attachment of PPI on the template was visually confirmed using optical and fluorescence microscopy (**Figure 4**). The PPI attachment is indicated by the development of black specks on the surface of the bubble in optical bright field images (**Figure 4D**). The clear demonstration of a green corona on the surface of the water droplet when fluorescence labeled PPI was used to create the emulsion (**Figure 4 H and I**) clearly established our hypothesis. Moreover, template-PPI droplets displayed corrugated and wrinkling surface probably due to the formation of a thin PU membrane via the interfacial reaction between isocyanate and encapsulated BD cargo. The membrane formation and speck deposition are deemed due to the formation of isocyanate (PPI) rich layer rather than the conventional interfacial reaction between the isocyanate dissolved in the oil phase and water in the dispersive phase. Thus, we established the formation of an “isocyanate-rich layer” around the template droplet which forms the basis of our bilayer capsule cell wall.

Key points:

- For the first time, we demonstrated the feasibility of developing an isocyanate-rich middle layer that in turn facilitates the formation of reinforcing the second layer.
- Proved our hypothesis using optical and fluorescence

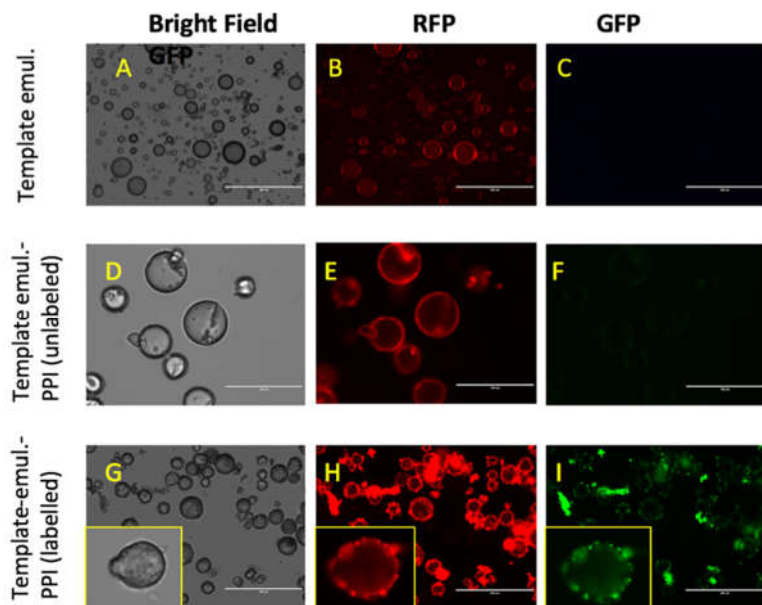
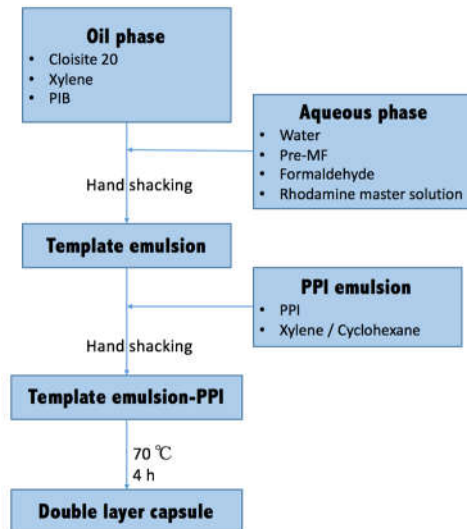


Figure 4 The characterization of the pre-emulsions. The optical and fluorescence image of the template droplet (A-C), template-PPI(D-F), and template-fluorescence labelled PPI (G-I) droplets.

microscopy, which showed the deposition of PPI on the droplet surface and plausible PU layer formation.

Stage b. Engineering PMF-PU double layer capsule

While the attachment of PPI and formation of a PU layer made it possible to have a capsule with stronger shell, they were not robust enough to withstand extreme processing conditions that the capsules will encounter while embedding in the resin. Therefore, an additional poly(melamine-formaldehyde) (PMF) internal layer was fabricated underneath the PU layer by a two-step chemistry^{23, 24}. Specifically, pre-MF oligomer was firstly synthesized in basic conditions (pH=9.25). Then, oligomers were cross-linked with each other at lower pH (pH=3.2) and mixed with the water phase during the preparation of the water-in-oil emulsion. During this process, Pre-MF grows in size, deposits on the (internal) interface of aqueous droplets, crosslink continually, and form PMF network eventually. Our study revealed that the formation of PU and PMF layers are not independent. We found that PMF skeleton will not form in the Pickering template without the concurrent PU layer formation as shown in **Figure 5**. Therefore, we hypothesize that a capsule PU template has its role in the formation of PMF. Moreover, the possible cross reactions between the PPI and the melamine, as well as the chain extender and formaldehyde may also contribute to form an internal layer between the PU and PMF. **Scheme 3** summarizes the entire process.



Scheme 3. Flowchart of capsule formation via PU external layer and PMF skeleton

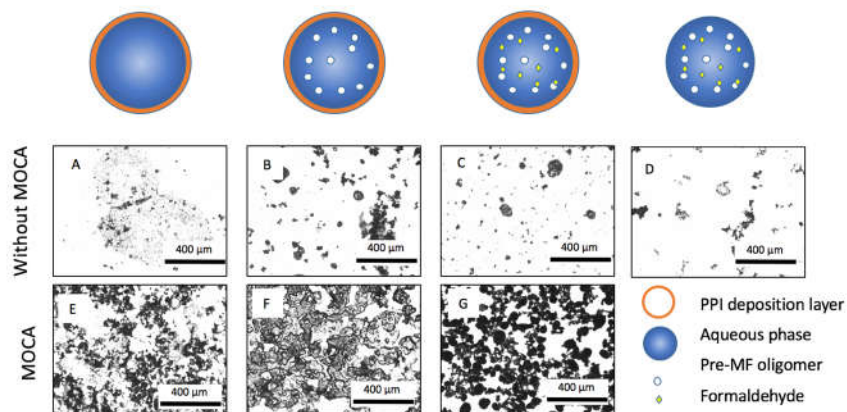


Figure 5. Shell forming factors analysis. Optical images of the dried capsule with different shell formation factors. Images are (A): template emulsion-PPI, (B): template emulsion-PPI with pre-MF in the aqueous phase, (C): (B) with excessive formaldehyde, and (D): template emulsion with pre-MF and excess formaldehyde. (E), (F) and (G) samples were prepared same as (A), (B), (C) respectively, but adding MOCA as a chain extender in the xylene phase. Results show that capsules can only be obtained in case (G), indicating MOCA, PPI, Pre-MF and excessive formaldehyde are critical factors to form robust capsules.

Characterization of the bilayer capsule: Improvements in the shell strength is the most direct observed consequence of adding the PMF lining. The collapse was prevented, and even after the drying process, a perfect spherical shape was maintained. We employed a fluorescent cargo (rhodamine B) to confirm the capsule formation and retention of the cargo inside the capsule.

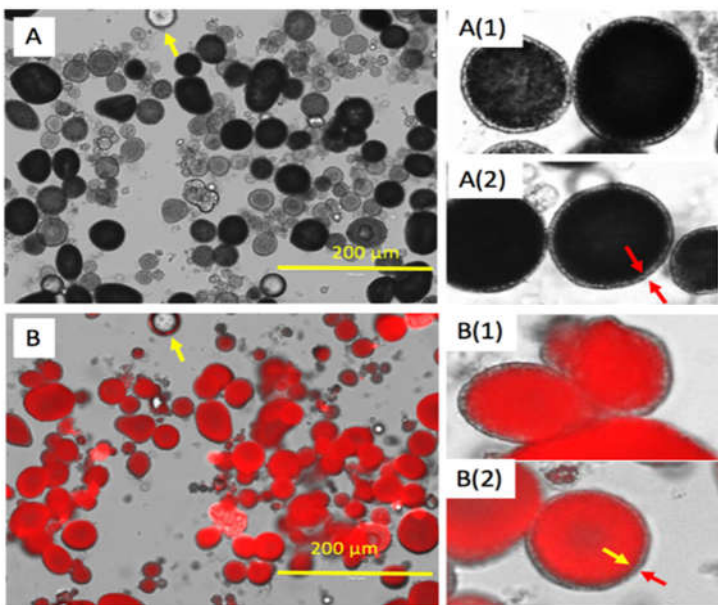


Figure 6 Microscopy of bi-layer capsule (suspension in xylene). Shell-core structure is visible under bright field. The rhodamine dye loaded in the capsule are visible under fluorescent microscopy. Arrows indicate the position of the shell

Microscopic analysis (**Figure 6**) confirmed that the dye is retained inside the container with a prominent observable thin layer of shell with distinct transmission. Cross-sectional SEM images of the capsule revealed an atypical “capsule” structure showing solid surface and porous occupied core (**Figure 7**). We assumed that, this dense surface layer and porous internal materials are PU and PMF respectively. To confirm this, we employed FT-IR spectroscopy which confirmed the presence of PMF and PU in the capsule (**Figure 8**). As a reference, spectra of cured aqueous phase (PMF, no PU) and single layer PU capsule (PU shell, no PMF) were also presented.

Key observations:

- PU-PMF double layer capsule exhibited robust shell, and proper dimensions for self-healing purpose. While the external PU layer function as the insulation, the internal PMF layer provided the mechanical support.
- The PU and PMF layers are not added up together in a simple and independent manner. PMF skeleton did not form in the Pickering template without the concurrent PU layer formation.

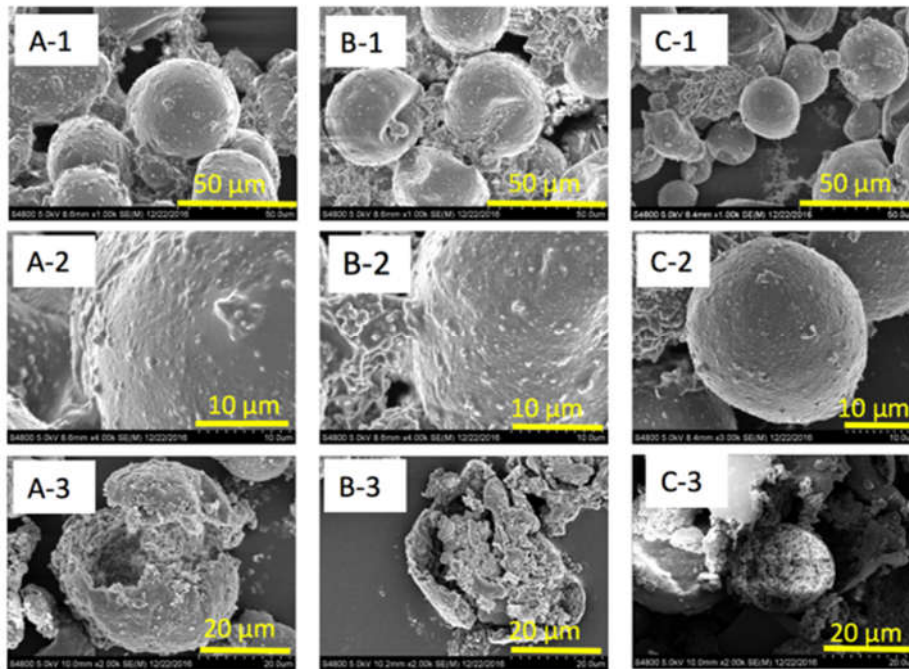


Figure 7 SEM images of the bi-layer capsules

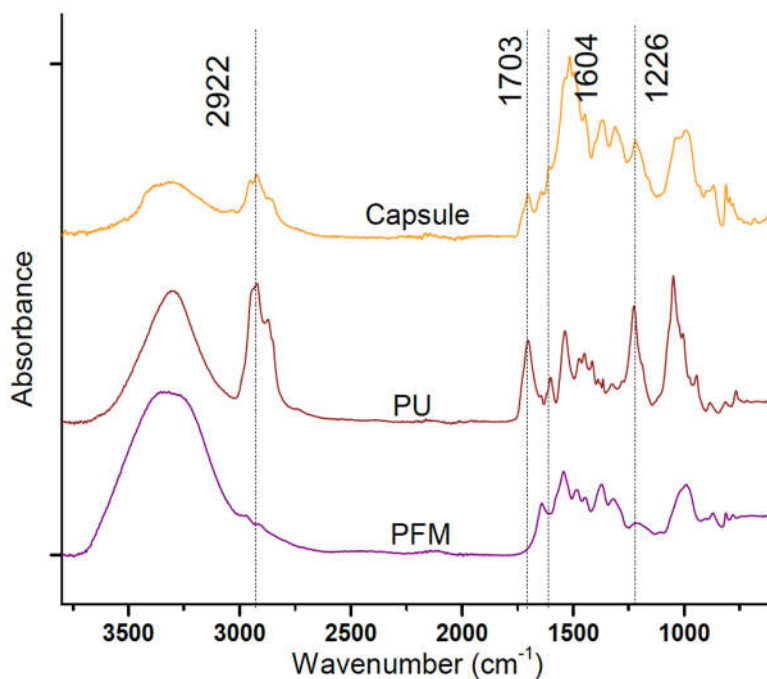


Figure 8 FTIR spectra of dry capsules. PU, PFM are references as internal and outer capsule materials

Studying the capsule permeability

The use of bi-layer capsule as self-healing agent, strongly depend on its ability to retain the payload. This in turn depends on the permeability of the capsule wall. Here, we performed a simple method to test its function of carrying the hydrophilic liquid. Capsules were completely dried on the glass slide at controlled condition (20°C, 35% humidity) for 7 days. Subsequently, the capsules were sandwiched between two glass slides and the top slide was pressed and moved parallel to the plane of the slide. This resulted in the release of payload that was observed in the microscope (**Figure 9**).

Key observations:

- PU-PMF double layer capsule held the hydrophilic payload under various processing conditions and released the formaldehyde payload upon application of external force.

Based on these results, we concluded that, the multilayer capsules are composed of a PU external layer, and a porous but stiffer PMF skeleton. The two components complemented each other in the encapsulation. The PMF skeleton, submerged in the cargo and provided mechanical support, and the external PU layer provided isolation against leakage.

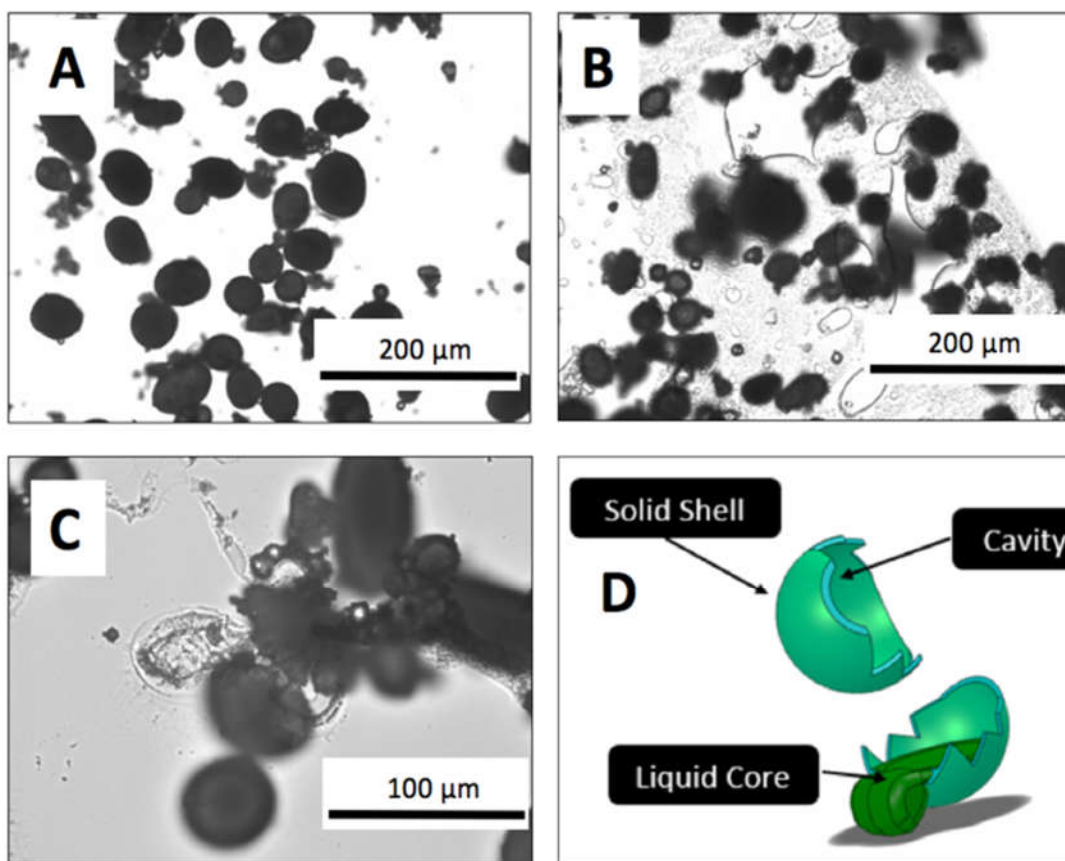


Figure 9 Aqueous cargo released after glass slide rolling. Optical images of (A): Complete dried capsules (sample G4); (B) and (C): Broken capsules; (D) schematic.

Part 2. Engineering of an AP-based cross-linked polymeric matrix (Self-funded study)

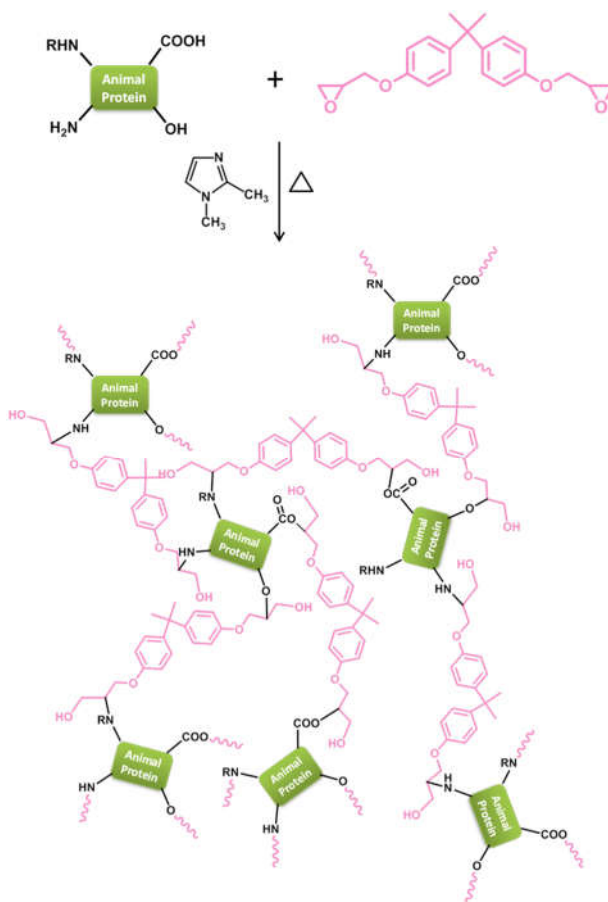
With the help of previous ACREC funding, we developed AP-Waterborne Polyurethane (WPU) hybrid polymers and also investigated the feasibility of AP-epoxy based thermoset materials. Particularly in the latter, due to the low compatibility between hydrophilic AP and hydrophobic epoxy, only partial curing was achieved and the desired mechanical properties were not obtained (when compared to the use of conventional hardeners). The addition of special additives such as BMI and HBP to the hybrid system led to significant improvement in the mechanical properties. However, for proposed applications e.g. in the automotive industry, considerable improvement is necessary via further refining of the reaction scheme.

Driven by our scientific curiosity and the understanding of high utility of a bio-based crosslinked epoxy resin, we continued our quest to innovate a strategy that can lead to fully functional AP-based thermoset systems. While use of waterborne epoxy is an option and demonstrated encouraging results, the utility and acceptability are inferior to conventional epoxy. Hence, we developed a novel catalytic strategy based on 1, 2-Dimethylimidazole (DMI), in the presence of which AP can completely crosslink conventional epoxy. The addition of highly renewable and environmentally friendly AP into matrix, the biocompatibility of the system is expected to improve. Hence, with a suite of attractive properties achieved by the addition of AP, the resultant hybrid material is expected to have wide applicability in diverse fields including the automotive industry.

Objective of part 2. The overall objective of the study is to develop high-strength, toughened, cross-linked thermosets and composites from proteinaceous materials from rendering industry and use it as matrix to incorporate self-healing capsules. Specific to this study, the goal is to develop a reaction methodology to involve as many functional groups in the reaction with epoxy during crosslinking reaction and exploit the abundance of functional groups in AP. Below we summarize the very latest and first-of-its-kind innovation where we mitigated the challenge to react hydrophilic AP with hydrophobic epoxy system through the use of a unique catalyst system that activates various functional groups in AP and triggers its reaction with the matrix. *To testify our methodology, we selected AP from feather meal since it has abundance of functional groups including, relatively, more number of thiol groups.* To simplify, the rest of document refers to feather-meal derived AP as AP.

Reaction flow:

Scheme 4 shows the flow of reaction leading to the development of AP-crosslinked epoxy matrix. In this reaction scheme, we used DMI as an activating catalyst that in the presence of heat initiates a ring opening reaction in epoxy resin and activated all potential functional groups in AP such as primary amine, secondary amine, carboxyl and hydroxyl groups. Such activated functional groups in the presence of a ring opened epoxies can trigger a self-cross linking reaction epoxies. This leads to the formation of highly cross-linked matrix and significantly improved mechanical properties.



Scheme 4. The process to prepare animal protein cross-linked thermoset

Results and discussion

Evidence of crosslinking: Figure 10 shows the FTIR spectrum of epoxy resins before and after curing with AP. Epoxy resins before the addition of AP (before curing), had a strong signature of epoxide ring vibration centered at 859 cm^{-1} . This is a signature showing the large abundance of epoxide ring in the resin. The addition of AP has demonstrated observable changes in the spectrum. Especially a reduction in intensity around 859 cm^{-1} corresponds to the opening-up of epoxy ring and concurrent reduction in the number of epoxy rings. This can be attributed to the reaction of epoxy rings with various functional groups in animal protein. In addition, a feature at 1728 cm^{-1} pointing towards the production of ester linkages confirming the crosslinking reaction.

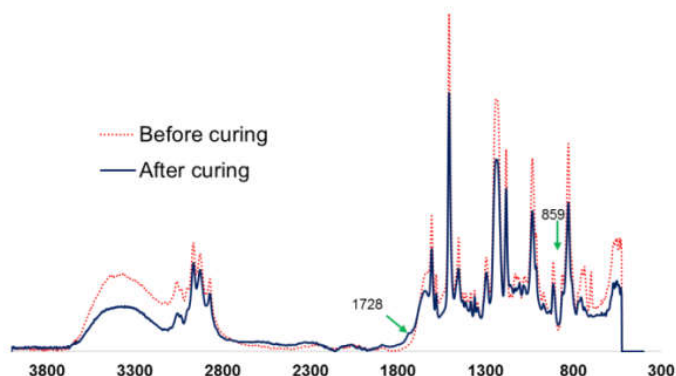


Figure 10. FTIR spectrum of the epoxy system before and after the crosslinking reaction with AP.

Evaluation of the mechanical properties: The crosslinked samples were analyzed for their mechanical performance. We use dynamic mechanical analysis (DMA) to characterize the mechanical properties.

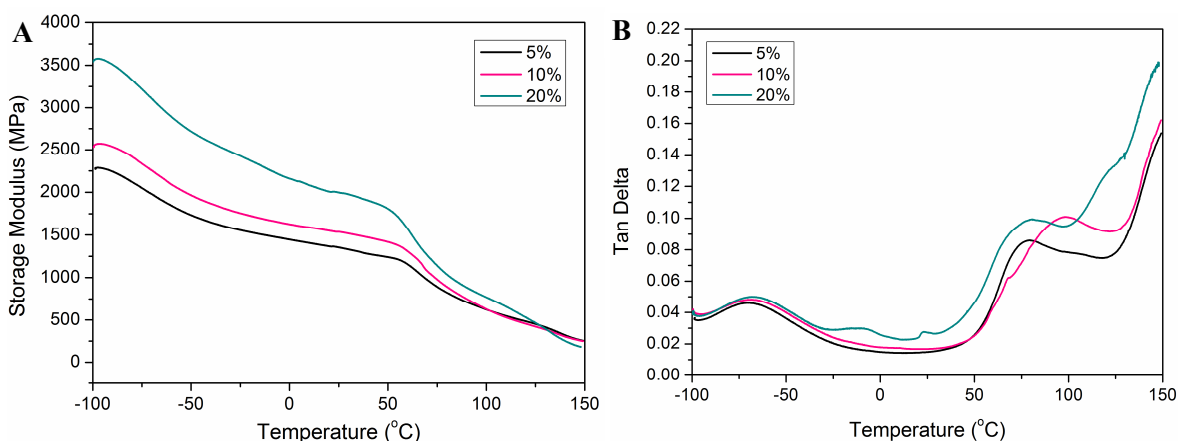


Figure 11. DMA results on AP- based cross-linked epoxy systems. A) storage modulus and B) Tan Delta.

For the DMA analysis, epoxy sample containing three different wt% of AP (i.e. 5, 10 and 20%) were fabricated. All three samples exhibited a monotonous decrease in storage modulus with the increase in temperature. This can be attributed to the softening of polymer chains by heat. However, it is important to note that addition of AP into epoxy resulted in an increase of storage modulus and with increase AP content, the storage modulus showed a proportional increase (Figure 11A). This can be attributed to the increased crosslinking of epoxy with increasing AP content. It is also worth noting that the effect of AP addition is only evident up to $125\text{ }^{\circ}\text{C}$, above which practically no change was observed. It confirmed that the animal protein functional groups are fully reacted during crosslinking reaction below $125\text{ }^{\circ}\text{C}$. Figure 11B depicts the variation of

loss factor ($\tan \delta$) as functions of temperature, at various AP content. The temperature at which the maximum loss factor is observed is considered as the glass transition temperature (T_g). According to **Figure 11 B**, 5%, 10% and 20% animal protein weight ratio had T_g values of 80°C, 100°C and 80°C respectively.

Key points:

- The concurrent emergence of peak at $\sim 1728 \text{ cm}^{-1}$ and the disappearance of peak around 859 cm^{-1} confirms the opening-up of epoxy rings and AP-induced cross-linking.
- DMA results showed corresponding increase in storage modulus with the addition of AP, again pointing to successful crosslinking of the epoxy matrix.

Part 3. Incorporation of developed microcapsules into engineered AP crosslinked epoxy matrix and test self-healing possibilities

While we overcame two critical challenges that prevent the use of AP-based self-healing resins namely; devising a carrier vehicle for hydrophilic payloads and engineering a resin system that is favourable chemistry for AP-assisted self-healing, we were only able to complete the very initial trials of the actual self-healing tests. The initial results are encouraging. Based on these studies, we submitted a proposal to conduct further research on the self-healing capabilities of AP-based matrices. The proposal is an amalgamation of the part 1 and 2 resulting in a novel AP encapsulated capsule which leverages the DMI catalysed crosslinking of epoxy resin to induce self-healing. We believe this is novel and carry immense potential, both for intellectual merits and broader and economic impacts of AP and the rendering industry.

Conclusion:

In this study, effective encapsulation of hydrophilic payload was accomplished by integrating two classical capsule formation chemistries, e.g. PU interfacial polymerization and PMF polycondensation deposition, via customized modifications. For PU shell formation, isocyanate rich pre-layer wrapping around each individual aqueous droplet was achieved by taking advantage of the insolubility of the custom-synthesized polymeric isocyanate, PPI, which in presence of a chain extender resulted in the formation of an impermeable PU outer layer. A further improvement in mechanical stability of the capsule was accomplished by incorporating the PMF lining under the PU layer. A special structure with dense external PU layer, and porous PMF skeleton was obtained and confirmed by SEM, fluoroscopy and FTIR. The resultant capsule was able to withstand the ambient drying process and was capable of holding the hydrophilic payload for long durations. In addition, we also discovered a novel DMI catalysed, AP-based crosslinking strategy which can be applied to any epoxy-based system. The high adaptability of the protocol is expected to attract large interest leading to high utility of AP in the composite industry.

Significance to the rendering industry:

The principle scientific benefit of this study is the use of animal proteins in the development of high-strength epoxy thermosets which can be applied to automotive coating/painting and other applications. Currently most of the curing chemistry is achieved by using synthetic amine-based hardeners. The developed DMI-AP-based curing chemistry can potentially replace the synthetic hardeners. In addition, the development of a stable capsule system which can encapsulate hydrophilic payload will catalyze further research on AP-based self-healing systems. Incorporation of such systems can help to enhance the service life of composites leading to

enhanced acceptability and utility for AP. This will generate high demand for AP leading to direct benefit to rendering industry.

Intellectual Property Development?

We are highly excited about the research outcomes of the project which is expected to deliver multiple patents. The ongoing research being novel and never attempted, the outputs are expected to have high intellectual value. While we already found multiple opportunities to develop intellectual property, we plan to explore these after a thorough search regarding the various patentable aspects of the project. One of the first opportunity will be the DMI-AP-based self-crosslinking of epoxy matrix. Further refinement and optimization of the process can lead to a bio-hardener based curing strategy that can be applied for various epoxy resins. Finally, development of microcapsule for hydrophilic payloads specifically targeting protein-based resin was achieved for the first time, which also mandates innovation.

Publications:

- 1) Yu, X., Zheng, T., Pilla, S., “Mechanical Properties of Waterborne Polyurethane Cross-linked by Rendered Animal Proteins,” Poster presentation at the *Society of Plastics Engineers ACCE Conference*, Novi, MI, September 7-9, 2016
- 2) Zheng, T., Yu, X., Pilla, S., “Mechanical and Moisture Sensitivity of Fully Bio-based Dialdehyde Carboxymethyl Cellulose Cross-linked Soy Protein Isolate Films,” *Carbohydrate Polymers*, 157, 1333-1340 (2017)

Outside funding: No outside funding has been pursued at this point. However, given the potentiality of the results, we intend to apply for funding to either National Science Foundation or the United States Department of Agriculture.

Future Work:

Given the potentiality of animal proteins, as we have observed in our preliminary studies, we intend to continue this research in developing an animal protein (AP)-based smart organic-inorganic hybrid self-healing system that not only imparts self-repairing capability to composites but also helps to visually validate the self-healing process. A proposal to this effect has been submitted for consideration by the ACREC governing committee.

Acknowledgments: My sincere thanks to my graduate students Xiaoyan Yu and Ting Zheng for their diligent efforts in the project. I would also like to thank my research scientist, Dr. Sreerprasad Sreenivasan for his insights on the project. Also, thanks to Kim Ivey for her kind assistance on the material characterization.

References

1. A. Schoth, K. Landfester and R. Munoz-Espi, *Langmuir*, 2015, **31**, 3784-3788.
2. S. Kuypers, S. K. Pramanik, L. D'Olieslaeger, G. Reekmans, M. Peters, J. D'Haen, D. Vanderzande, T. Junkers, P. Adriaensens and A. Ethirajan, *Chemical Communications*, 2015, **51**, 15858-15861.
3. H. N. Yow and A. F. Routh, *Soft Matter*, 2006, **2**, 940-949.
4. H. Yi, Y. Yang, X. Gu, J. Huang and C. Wang, *Journal of Materials Chemistry A*, 2015, **3**, 13749-13757.
5. E. Koh, S.-Y. Baek, N.-K. Kim, S. Lee, J. Shin and Y.-W. Kim, *New Journal of Chemistry*, 2014, **38**, 4409-4419.
6. J. Yang, M. W. Keller, J. S. Moore, S. R. White and N. R. Sottos, *Macromolecules*, 2008, **41**, 9650-9655.
7. D. A. McIlroy, B. J. Blaiszik, M. M. Caruso, S. R. White, J. S. Moore and N. R. Sottos, *Macromolecules*, 2010, **43**, 1855-1859.
8. O. Velez and K. Nagayama, *Langmuir*, 1997, **13**, 1856-1859.
9. E. Donath, G. B. Sukhorukov, F. Caruso, S. A. Davis and H. Möhwald, *Angewandte Chemie International Edition*, 1998, **37**, 2201-2205.
10. D. Voorn, W. Ming and A. Van Herk, *Macromolecules*, 2006, **39**, 2137-2143.
11. C. Yeom, S. Oh, J. Rhim and J. Lee, *Journal of applied polymer science*, 2000, **78**, 1645-1655.
12. J. Li, A. D. Hughes, T. H. Kalantar, I. J. Drake, C. J. Tucker and J. S. Moore, *ACS Macro Letters*, 2014, **3**, 976-980.
13. J. D. Rule, N. R. Sottos and S. R. White, *Polymer*, 2007, **48**, 3520-3529.
14. R. C. Hayward, A. S. Utada, N. Dan and D. A. Weitz, *Langmuir*, 2006, **22**, 4457-4461.
15. Y. Yang, Y. Ning, C. Wang and Z. Tong, *Polymer Chemistry*, 2013, **4**, 5407-5415.
16. A. Samanta, M. Tesch, U. Keller, J. r. Klingauf, A. Studer and B. J. Ravoo, *Journal of the American Chemical Society*, 2015, **137**, 1967-1971.
17. S. A. Bon and T. Chen, *Langmuir*, 2007, **23**, 9527-9530.
18. S. B. Jagtap, M. S. Mohan and P. G. Shukla, *Polymer*, 2016, **83**, 27-33.
19. S. Torza and S. Mason, *Journal of Colloid and Interface Science*, 1970, **33**, 67-83.
20. Y. Wang, J. He, C. Liu, W. H. Chong and H. Chen, *Angewandte Chemie International Edition*, 2015, **54**, 2022-2051.
21. J. W. Kim, J. Cho, J. Cho, B. J. Park, Y. J. Kim, K. H. Choi and J. W. Kim, *Angewandte Chemie International Edition*, 2016.
22. A. Loxley and B. Vincent, *Journal of colloid and interface science*, 1998, **208**, 49-62.
23. M. Palanikkumaran, K. K. Gupta, A. K. Agrawal and M. Jassal, *Journal of applied polymer science*, 2009, **114**, 2997-3002.
24. H. Lee, S. Lee, I. Cheong and J. Kim, *Journal of microencapsulation*, 2002, **19**, 559-569.
25. W.-j. Luo, W. Yang, S. Jiang, J.-m. Feng and M.-b. Yang, *Polymer degradation and stability*, 2007, **92**, 1359-1364.
26. Y. Long, D. York, Z. Zhang and J. A. Preece, *Journal of Materials Chemistry*, 2009, **19**, 6882-6887.
27. T. Zheng, X. Yu and S. Pilla, *Carbohydrate Polymers*, 2017, **157**, 1333-1340.